Three-dimensional changes of the zygomaticomaxillary complex after mini-implant assisted rapid maxillary expansion

Kyeong-Tae Song,[a] Jae Hyun Park,[b,c] Won Moon,[d] Jong-Moon Chae,[e,f] and Kyung-Hwa Kang[g]
Iksan and Seoul, South Korea, Mesa, Ariz, and Los Angeles, Calif

Introduction: The aim of this study was to investigate 3-dimensional changes of the zygomaticomaxillary complex (ZMC) after mini-implant assisted rapid maxillary expansion (MARME). **Methods:** A total of 15 pairs of cone-beam computed tomography 3-dimensional images taken before expansion (T0) and after expansion (T1) were analyzed by measuring changes in the coordinates of the landmarks of the ZMC. **Results:** Changes in the x coordinates of the landmarks showed significant expansion ($P < 0.01$) and greater expansion at the lower than upper portion of the ZMC ($P < 0.05$) in the transverse dimension. All y coordinates of the landmarks except the jugal point (J) showed forward displacement ($P < 0.05$), and the z coordinates of ANS, PNS, Alare, A, and ectocanine showed downward displacement ($P < 0.01$) in the sagittal and vertical dimensions. Also, z coordinates of the landmarks that were closer to the midsagittal plane and in a more posterior portion of the ZMC displaced further downward ($P < 0.05$). SNA and ANB angles increased ($P < 0.05$ and $P < 0.001$, respectively) and the SNB angle decreased ($P < 0.01$). There was a significant correlation between changes in the x coordinates of the ectomolare and ectocanine and the amount of expansion measured from the center of resistance of the maxillary first molars (CR6; $P < 0.05$). There was no significant correlation between the amount of CR6 expansion and changes in y and z coordinates of the landmarks. **Conclusions:** 3-Dimensional changes of the ZMC after MARME showed expansion in a pyramidal shape from the coronal view, downward and forward displacement from the sagittal view, and parallel palatal expansion from the axial view. These findings might be useful for understanding skeletal expansion patterns using MARME. (Am J Orthod Dentofacial Orthop 2019;156:653-62)

In the 1960s, Haas[1] reported rapid palatal expansion (RPE) in growing children. Since then, a variety of palatal expansion appliances have been developed and used widely to correct the transverse maxillary deficiency,[2-4] but the skeletal effects can be reduced or even eliminated as the resistance against expansion increases with the skeletal maturity of the patient.[5,6] Surgically assisted rapid palatal expansion was introduced to overcome the transverse maxillary deficiency in skeletally mature patients.[7] However, owing to high risks and costs, surgical complexity, and morbidity, many patients rejected a surgical intervention. Recently, mini-implant assisted rapid palatal expansion (MARPE) has been suggested as an alternative to surgically assisted rapid palatal expansion in adults to open midpalatal suture.[8,9] Orthodontic mini-implants have been proposed as a skeletal anchorage for RPE to provide more orthopedic expansion while reducing undesirable side effects such as dentoalveolar tipping, periodontal dehiscence, and marginal bone loss.[8,10]

[a]Resident, Department of Orthodontics, School of Dentistry, University of Wonkwang, Iksan, South Korea.
[b]Professor and chair, Postgraduate Orthodontic Program, Arizona School of Dentistry & Oral Health, A.T. Still University, Mesa, Ariz.
[c]International Scholar, Graduate School of Dentistry, Kyung Hee University, Seoul, South Korea.
[d]Associate professor, Center for Health Sciences, Section of Orthodontics, School of Dentistry, University of California, Los Angeles, Calif.
[e]Professor, Department of Orthodontics, School of Dentistry, University of Wonkwang, Wonkwang Dental Research Institute, Iksan, South Korea.
[f]Visiting Scholar, Postgraduate Orthodontic Program, Arizona School of Dentistry and Oral Health, A.T. Still University, Mesa, Ariz.
[g]Professor, Department of Orthodontics, School of Dentistry, University of Wonkwang, Wonkwang Dental Research Institute, Iksan, South Korea.
All authors have completed and submitted the ICMJE Form for Disclosure of Potential Conflicts of Interest, and none were reported.
Address correspondence to: Kyung-Hwa Kang, Department of Orthodontics, School of Dentistry, Wonkwang University, 460 Iksandae-ro, Iksan-si, 54538, South Korea; e-mail, pigtail@wonkwang.ac.kr.
Submitted, September 2018; revised and accepted, November 2018.
0889-5406/$36.00

https://doi.org/10.1016/j.ajodo.2018.11.019

Previous studies[11–13] suggested a forward and downward displacement of the maxilla following expansion in growing patients, but there are disagreements regarding the rotation of the palatal plane. Chung and Font[11] reported that the maxilla was displaced forward and downward after expansion with parallel downward movement of the palatal plane. Habeeb et al[12] described how the maxilla was displaced forward and downward after expansion with clockwise rotation of the palatal plane. Silva et al[13] reported counterclockwise rotation of the palatal plane with forward and downward displacement of the maxilla after expansion.

Yılmaz et al[14] described parallel expansion of the maxilla and an increase in SNA angle without change in vertical dimension after mini-implant assisted rapid maxillary expansion (MARME). The study used 2-dimensional lateral and anteroposterior cephalograms to evaluate the skeletal effects. However, measurements using conventional 2-dimensional radiographs are limited, and minor changes were barely identifiable because of overlapping of the anatomical structures. In 2017, Park et al[10] reported on the 3-dimensional skeletal and dentoalveolar changes of the maxilla after MARPE using cone-beam computed tomography (CBCT) images. However, there are few studies about the expansion pattern of the zygomaticomaxillary complex (ZMC).

Therefore, the aim of this study was to evaluate 3D skeletal and dentoalveolar changes of the ZMC after MARME by measuring the changes in the x, y, and z coordinates of the landmarks of the ZMC using CBCT images.

MATERIAL AND METHODS

Subjects, eligibility criteria, and CBCT

This retrospective study was approved by the institutional review board of the Wonkwang University (WKDIRB201709-01). A total of 15 patients (mean age, 18.8 years; range, 9.2-24.5 years; 5 males, 10 females) were selected from Wonkwang University Dental Hospital in Iksan and Sanbon, South Korea, to be included in this study. The inclusion criteria were as follows: less than 5 mm of difference between maxillary and mandibular intermolar width or less than −2 mm difference between the distance of the center of resistance of the first molars in maxillary and mandibular arches, success in opening the midpalatal suture, and activating the expander according to our expansion protocol. To define the success when opening the midpalatal suture, periapical radiographs were taken when the diastema was made during expansion. Exclusion criteria included the following: failure to open the midpalatal suture, patients who were already undergoing orthodontic or orthopedic treatment, excessively long intervals (>100 days) between before expansion (T0) and after expansion (T1), and patients who had just completed orthognathic surgery. The mean duration of expansion was approximately 35 days with a range from 13 to 73 days.

In this study, MARME appliance (MSE; BioMaterials Korea, Seoul, South Korea) was used on all patients for rapid maxillary expansion (RME). Type I appliances expand by 0.8 mm in 4 turns, but type II appliances expand by 0.8 mm in 6 turns. Type II appliances were used in this study. The body size of the MARME appliance is 13.5 × 14.5 mm. It is positioned in the paramidsagittal area between the maxillary first molars. MSE has 4 holes and 4 arms that are soldered to the bands of the maxillary first permanent molars. Four 1.5 × 11.0 mm mini-implants are used to fenestrate the palatal base and nasal base to generate greater expansive skeletal forces (Fig 1). The maximum amount of expansion possible with the appliance used in this study was 8.0 mm. The activation rate was 1 turn per day for early teens (<15 years), 2 turns per day for late teens (≥ 15 years), and 4 turns per day for adult patients older than 20 years. Once the diastema was identified, the activation rate was changed to 2 turns per day for all patients, regardless of age.[15]

To evaluate the skeletal changes of the ZMC after MARME, CBCT images were taken of each subject before expansion (T0) and after expansion (T1). When taking CBCT images, the CBCT scanner (Alphard-3030; Asahi Roentgen Ind, Kyoto, Japan) was set at 80 kVp and 7.0 mA for adults and 80 kVp and 3.0 mA for adolescents, and the images were gained for 17 seconds, with a voxel size of 0.39 mm as cranial mode. All patients were instructed to be seated upright in such a manner that the Frankfort horizontal plane of their heads was parallel to the floor. Their heads were fixed using both a chincup and ear rod. After the images were taken, they were imported as digital imaging and communications in medicine files by using the INFINITT PACS software program (INFINITT Healthcare Co, Ltd, Seoul, South Korea).

Measurements

All CBCT images were reorientated using OnDemand3D software (Cybermed, Seoul, South Korea),[16] then the landmarks were traced, and each landmark was given its own coordinates in 3 dimensions. After tracing both T0 and T1 CBCT images of each individual subject, they were superimposed on the basis of anterior cranial base using the same software program (OnDemand3D) described above. In this study, some landmarks

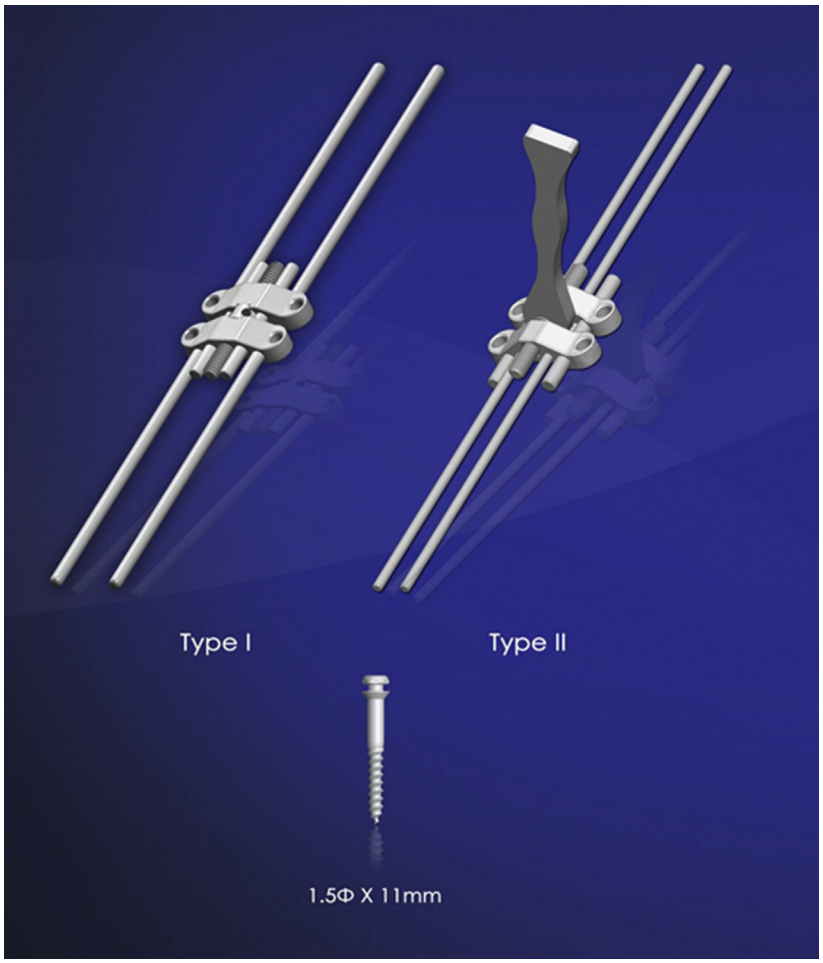

Fig 1. The MARME appliance (MSE) used in this study. In this study, a type II appliance was used.

were set up for evaluation of displacement of the ZMC after MARME. The name and definition of each landmark of the ZMC has been detailed in Table I and they are shown in Fig 2.

Results were measured by calculating the difference between T0 and T1 for each coordinate of the landmarks. The x-axis was in the transverse dimension, the y-axis was in the anteroposterior dimension and the z-axis was in the vertical dimension. The plus and minus directions were indicated along the 3 axes in Fig 3. The points on the left and right sides of ANS, PNS, and A were located at the same point before expansion. Therefore, they were defined as "midline landmarks." The points on the left and right sides of Z, Alare, J, ectomolare, ectocanine, and CR6 were located at each side of the ZMC. Therefore, they were defined as "bilateral landmarks." The displacement along the 3 axes was calculated as the mean value of the displacement of the left and right landmarks. Absolute values were used for the x coordinate of the bilateral landmarks on the right side and the displacement to the right side in the transverse dimension to calculate mean values.

Statistical analysis

A power analysis using G*Power (version 3.1.9.2; Franz Faul, Christan-Albrechts-Universitat, Kiel, Germany) was used to determine the sample size required for this study. It was determined that 15 subjects would be needed to provide a power of 0.82 and 2-tailed α value of 0.05.

The tracing and superimposition process of all CBCT images was done by 1 examiner (K.T.S.) to minimize measurement error. Six randomly selected CBCT images were traced and superimposed once more after a 4-week interval to evaluate the intraclass reliability. The intraclass correlation coefficient was from 0.806 to 0.929, which is considered to be excellent for intraclass reliability testing.

Table I. Landmarks of the zygomaticomaxillary complex used in this study

Landmarks	*Definition*
ANS	A pointed projection at the anterior extremity of the intermaxillary suture
PNS	Medial end of the posterior border of the horizontal plate of palatine bone
Z	The most lateral point of the zygomatic arch in the coronal plane
Alare	The most inferolateral point of the nasal aperture in the coronal plane
J	The intersection of the tuberosity of the maxilla and zygomatic buttress
A	The deepest point of the anterior contour of the maxillary alveolar process in the midsagittal plane
Ectocanine	The most lateral point of the alveolar ridge at the level of center of the maxillary canine
Ectomolare	The most lateral point of the alveolar ridge at the level of the maxillary first molar
CR6	The center of resistance of the maxillary first molar

Bilateral skeletal landmarks: Z, alare, J, ectocanine, and ectomolare.
Unilateral skeletal landmarks: ANS, PNS, and A.

The Shapiro-Wilk test was used to verify the normality of each data group. After identifying the normality of data, paired *t* tests were used for comparison of changes in the x, y, and z coordinates of the landmarks between left and right sides, and for the evaluation of changes in each coordinate and SNA, SNB, and ANB angles between T0 and T1. A 1-way ANOVA result with Tukey post-hoc test was used for comparison of changes in each coordinate between the landmarks. A Pearson correlation test was done to identify the correlation between the amount of expansion measured from the center of resistance of the maxillary first molars and the amount of change in the x, y, and z coordinates of the landmarks. All statistical analysis was performed using SPSS version 12.0 software (SPSS, Chicago, Ill).

RESULTS

Changes in x, y, and z coordinates of the landmarks

There was no significant difference in the comparison of changes in the x, y, and z coordinates of the landmarks between the left and right sides ($P > 0.05$), except for changes in the x coordinates of alare and ectocanine ($P < 0.05$; Table II).

The x coordinates of ANS, PNS, Z, alare, J, A, ectomolare, ectocanine, and CR6 increased by 1.06, 0.97, 0.45, 1.13, 1.17, 0.98, 1.68, 1.73, and 2.53 mm, respectively ($P < 0.01$; Table III). The y coordinates of ANS, PNS, Z, alare, A, ectocanine, ectomolare, and CR6 decreased by 0.34, 0.63, 0.54, 0.32, 0.72, 0.63, 0.47, and 0.51 mm, respectively ($P < 0.05$; Table IV). The z coordinates of ANS, PNS, alare, A, and ectocanine decreased by 0.39, 1.15, 0.56, 0.88, and 0.59 mm, respectively ($P < 0.01$; Table V), but the z coordinates of J increased by 0.31 mm ($P < 0.05$; Table V).

Comparison of changes in each coordinate between the landmarks

The results showed statistically significant differences of the changes in each coordinate between the landmarks ($P < 0.001$; Table III, $P < 0.01$; Table IV, $P < 0.001$; Table V, respectively).

The x coordinates of CR6 (2.53 ± 0.67 mm) showed the greatest increase among the landmarks ($P < 0.001$; Table III) followed by ectocanine and ectomolare (1.73 ± 0.79 and 1.68 ± 0.85 mm, respectively), J, alare,

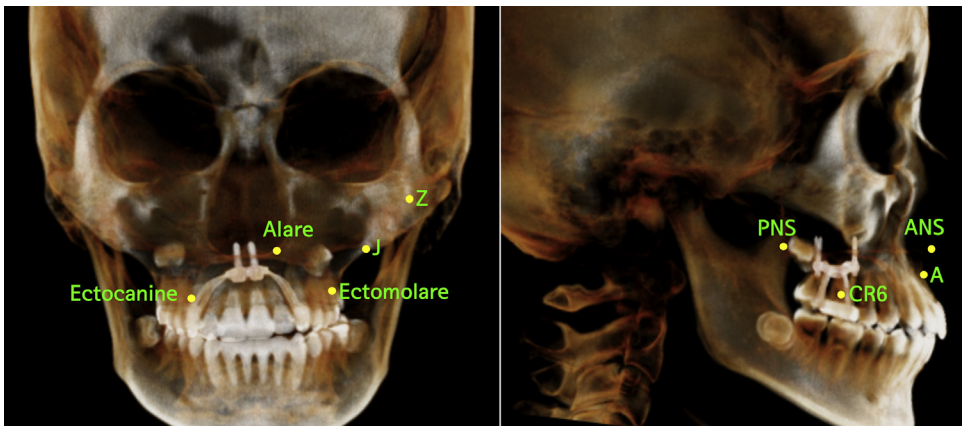

Fig 2. Landmarks of the zygomaticomaxillary complex used in this study: bilateral skeletal landmarks, Z, alare, J, ectocanine, and ectomolare; unilateral skeletal landmarks, ANS, PNS, and A.

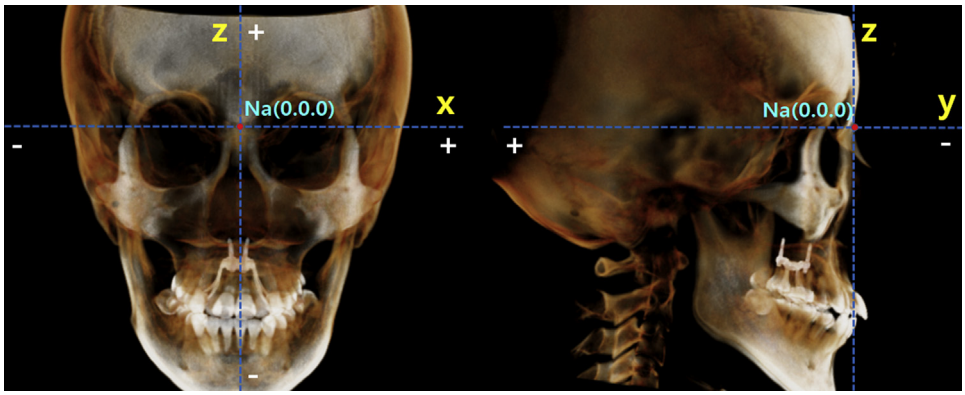

Fig 3. The plus and minus values along the 3 axes used in this study. The coordinates of the landmarks were assigned according to the nasion (0, 0, 0). For the x-axis, landmarks on the left side was a (+) value and right side was a (−) value. For the y-axis, landmarks located posterior to the nasion was a (+) value and anterior to nasion was a (−) value. For the z-axis, landmarks located superior to the nasion was a (+) value and inferior to the nasion was a (−) value. Displacement leftward, backward, and upward was a (+) value, and displacement rightward, forward, and downward was a (−) value.

Table II. Comparison of changes in x, y, and z coordinates of the landmarks between left and right sides

Landmark	*Coordinates*	*ΔT1-T0 (left)*	*ΔT1-T0 (right)*	*Differences*	P *value*
ANS	x	1.06 ± 0.48	1.07 ± 0.61	0.01 ± 0.20	0.961
	y	0.32 ± 0.17	0.34 ± 0.17	0.02 ± 0.06	0.767
	z	0.45 ± 0.35	0.47 ± 0.37	0.02 ± 0.13	0.908
PNS	x	0.95 ± 0.56	1.02 ± 0.33	0.07 ± 0.17	0.656
	y	0.69 ± 0.48	0.70 ± 0.49	0.01 ± 0.18	0.943
	z	1.09 ± 0.41	1.11 ± 0.43	0.02 ± 0.15	0.900
Z	x	0.56 ± 0.40	0.33 ± 0.83	0.23 ± 0.24	0.447
	y	−0.40 ± 0.80	−0.67 ± 1.43	0.27 ± 0.42	0.601
	z	0.22 ± 0.74	−0.19 ± 1.00	0.41 ± 0.31	0.265
Alare	x	0.91 ± 1.05	1.41 ± 1.11	0.51 ± 0.39	0.034*
	y	−0.30 ± 0.71	−0.34 ± 0.57	0.04 ± 0.24	0.873
	z	−0.61 ± 0.77	−0.54 ± 0.58	0.07 ± 0.24	0.640
J	x	1.09 ± 0.84	1.26 ± 0.98	0.17 ± 0.33	0.646
	y	0.05 ± 0.99	−0.04 ± 0.66	0.10 ± 0.31	0.742
	z	0.25 ± 0.52	0.30 ± 0.49	0.05 ± 0.18	0.577
A	x	0.90 ± 0.58	1.06 ± 0.70	0.16 ± 0.23	0.431
	y	0.67 ± 0.36	0.67 ± 0.35	0.01 ± 0.13	0.972
	z	0.99 ± 0.72	0.99 ± 0.75	0.00 ± 0.27	0.994
Ectomolare	x	1.64 ± 1.10	1.72 ± 0.79	0.07 ± 0.35	0.748
	y	−0.61 ± 0.73	−0.32 ± 0.65	0.29 ± 0.25	0.307
	z	−0.18 ± 0.52	−0.24 ± 0.63	0.06 ± 0.19	0.952
Ectocanine	x	1.50 ± 0.75	1.96 ± 0.96	0.46 ± 0.31	0.020*
	y	−0.60 ± 0.55	−0.65 ± 0.70	0.05 ± 0.23	0.807
	z	−0.69 ± 0.55	−0.59 ± 0.49	0.09 ± 0.21	0.624
CR6	x	2.49 ± 0.82	2.57 ± 0.73	0.08 ± 0.28	0.699
	y	−0.66 ± 0.43	−0.53 ± 0.39	0.14 ± 0.63	0.416
	z	−0.34 ± 0.22	−0.31 ± 0.27	0.03 ± 0.32	0.719

Data are presented as mean ± standard deviation.
Paired *t* tests were performed because of the normality of the data.
*$P < 0.05$.

Table III. Changes in x coordinates of the landmarks of the zygomaticomaxillary complex before (T0) and after (T1) expansion and comparison between the landmarks (n = 15; mm)

	T0		*T1*	*ΔT1-T0*	P *value*
ANS	−0.17 ± 0.84	Left	0.89 ± 0.98	1.06 ± 0.39[b]	0.000[†]
		Right	−1.23 ± 1.05		
PNS	−0.57 ± 0.95	Left	0.34 ± 0.94	0.97 ± 0.38[b]	0.000[†]
		Right	−1.59 ± 1.09		
Z	55.74 ± 3.41		56.19 ± 3.38	0.45 ± 0.31[a]	0.000[†]
Alare	8.65 ± 1.13		9.78 ± 1.34	1.13 ± 1.02[b]	0.006[*]
J	39.74 ± 1.73		40.91 ± 1.68	1.17 ± 0.58[b]	0.000[†]
A	−0.30 ± 0.76	Left	0.60 ± 1.04	0.98 ± 0.50[b]	0.000[‡]
		Right	−1.36 ± 0.95		
Ectomolare	29.30 ± 1.86		30.98 ± 1.75	1.68 ± 0.85[c]	0.000[†]
Ectocanine	17.40 ± 1.99		19.13 ± 2.04	1.73 ± 0.79[c]	0.000[†]
CR6	22.94 ± 1.71		25.47 ± 1.87	2.53 ± 0.67[d]	0.000[†]
P value				0.000[‡]	

Data are presented as mean ± standard deviation.
Paired *t* tests were performed because of the normality of the data.
One-way ANOVA were performed because of the normality of the data.
Tukey honest significant difference test was performed; subgroups for $\alpha = 0.05$.
For midline landmarks, average value of the amount of expansion of both sides was used.
Different characters represent statistical difference (a<b<c<d).
Midline landmarks: ANS, PNS, and A; bilateral landmarks: Z, alare, J, ectomolare, ectocanine, and CR6.
Left side (+); right side (−). Absolute value was used for the bilateral landmarks on the right side.
[*]*P* <0.01; [†]*P* <0.001; [‡]*P* <0.001.

Table IV. Changes in y coordinates of the landmarks of the zygomaticomaxillary complex before (T0) and after (T1) expansion and comparison between the landmarks (n = 15; mm)

	T0	*T1*	*ΔT1-T0*	P *value*
ANS	−4.74 ± 4.60	−5.08 ± 4.64	−0.34 ± 0.23[a,b]	0.000[‡]
PNS	44.12 ± 3.50	43.49 ± 3.65	−0.63 ± 0.57[a]	0.001[†]
Z	24.70 ± 3.30	24.17 ± 3.14	−0.54 ± 0.61[a,b]	0.004[†]
Alare	4.21 ± 3.64	3.89 ± 3.84	−0.32 ± 0.47[a,b]	0.021[*]
J	19.77 ± 2.27	19.77 ± 2.49	−0.01 ± 0.63[b]	0.965
A	−1.65 ± 4.51	−2.37 ± 4.47	−0.72 ± 0.39[a]	0.000[‡]
Ectocanine	2.31 ± 4.90	1.68 ± 5.04	−0.63 ± 0.50[a]	0.000[‡]
Ectomolare	21.42 ± 4.57	20.95 ± 4.26	−0.47 ± 0.45[a,b]	0.001[†]
CR6	23.15 ± 4.63	22.65 ± 4.60	−0.51 ± 0.31[a,b]	0.000[‡]
P value			0.004[§]	

Data are presented as mean ± standard deviation.
Paired *t* tests were performed because of the normality of the data.
One-way ANOVA were performed because of the normality of the data.
Tukey honest significant difference test was performed; subgroups for $\alpha = 0.05$.
(−) Anterior direction.
Different characters represent statistical difference (a<b).
(+) Posterior direction.
[*]*P* <0.05; [†]*P* <0.01; [‡]*P* <0.001; [§]*P* <0.01.

ANS, and PNS (1.17 ± 0.58, 1.13 ± 1.02, 1.06 ± 0.39, and 0.97 ± 0.38 mm, respectively) and Z (0.45 ± 0.31 mm). There was a statistically significant difference (*P* <0.01; Table IV) between the decrease in the y coordinates of A, PNS, and ectocanine (−0.72 ± 0.39, −0.63 ± 0.57, and −0.63 ± 0.50 mm, respectively) and the increase in y coordinates of J (0.01 ± 0.63 mm). There was a statistically significant difference between the decrease in the z coordinate of PNS (−1.15 ± 0.41 mm), alare (−0.56 ± 0.65 mm) and ANS (−0.39 ± 0.41 mm). The z coordinate of J increased (0.31 ± 0.41 mm) rather than decreasing (*P* <0.001; Table V). There was a

Table V. Changes in z coordinates of the landmarks of the zygomaticomaxillary complex before (T0) and after (T1) expansion and comparison between the landmarks (n = 15; mm)

	T0	*T1*	*ΔT1-T0*	P *value*
ANS	−51.99 ± 2.94	−52.38 ± 2.80	−0.39 ± 0.41^{b,c,d}	0.003†
PNS	−52.65 ± 3.87	−53.79 ± 3.88	−1.15 ± 0.41^{a}	0.000‡
Z	−33.51 ± 3.55	−33.45 ± 3.30	−0.06 ± 0.61^{d,e}	0.702
Alare	−49.96 ± 3.08	−50.52 ± 2.91	−0.56 ± 0.65^{b,c}	0.005†
J	−41.20 ± 2.80	−40.89 ± 2.80	−0.31 ± 0.41^{e}	0.011*
A	−57.47 ± 3.81	−58.35 ± 3.57	−0.88 ± 0.69^{a,b}	0.000‡
Ectocanine	−64.22 ± 4.03	−64.81 ± 3.98	−0.59 ± 0.34^{a,b,c}	0.000‡
Ectomolare	−65.00 ± 4.44	−65.19 ± 4.46	−0.19 ± 0.51^{c,d,e}	0.174
CR6	−67.58 ± 5.36	−67.52 ± 5.37	−0.05 ± 0.44^{d,e}	0.650
P value			0.000§	

Data are presented as mean ± standard deviation.
Paired *t* tests were performed because of the normality of the data.
One-way ANOVA were performed because of the normality of the data.
Tukey honest significant difference test was performed; subgroups for $\alpha = 0.05$.
(−) Inferior direction.
Different characters represent statistical difference (a<b<c<d<e).
(+) Superior direction.
$^{*}P < 0.05$; $^{\dagger}P < 0.01$; $^{\ddagger}P < 0.001$; $^{\S}P < 0.001$.

statistically significant difference between the change in the z coordinate of PNS and ANS (−1.15 ± 0.41 and 0.39 ± 0.41 mm, respectively, $P < 0.001$; Table V).

Changes in SNA, SNB, and ANB angles

The SNA angle increased by 0.46° ($P < 0.05$), the SNB angle decreased by 0.55° ($P < 0.01$), and the ANB angle increased by 1.01° ($P < 0.001$; Table VI).

Correlation between the amount of expansion of CR6 and changes in the x, y, and z coordinates of the landmarks

There were significant, positive correlations between the amount of expansion of CR6 and changes in the x coordinates of the ectomolare and ectocanine located at the alveolar bone level with coefficients of 0.601 ($P < 0.05$) and 0.779 ($P < 0.001$), respectively (Table VII). No significant correlation was found between the amount of CR6 expansion and the changes in the y and z coordinates of all the other landmarks, except for the y coordinates of the alare with a coefficient of 0.690 ($P < 0.01$; Table VII).

DISCUSSION

In this study, the x coordinates of the lower landmarks increased more than the upper landmarks of the ZMC, and palatal expansion was similar in anteroposterior portion. The skeletal expansion pattern of the ZMC had a pyramidal shape based on the center being near the frontonasal suture in the coronal view, and forward and downward displacement in the sagittal view as described in previous studies (Fig 4).[10,17,18]

Table VI. Changes (°) in SNA, SNB, and ANB angles (n = 15)

	T0	*T1*	*ΔT1-T0*	P *value*
SNA	80.96 ± 4.80	81.43 ± 4.66	0.46 ± 0.75	0.031*
SNB	79.42 ± 4.02	78.88 ± 4.10	−0.55 ± 0.62	0.004†
ANB	1.54 ± 1.67	2.55 ± 1.70	1.01 ± 0.68	0.000‡

Data are presented as mean ± standard deviation.
Paired *t* tests were performed because of the normality of the data.
$^{*}P < 0.05$; $^{\dagger}P < 0.01$; $^{\ddagger}P < 0.001$.

The skeletal expansion pattern of the ZMC in this study would depend on the center of resistance of the ZMC and the point of application of the force generated by the expander as reported by Lee et al.[19] However, Braun et al[20] and Baldawa and Bhad[21] reported that the center of rotation during the initial displacement of the dentomaxillary complex was on the frontonasal suture, whereas Gautam et al[22] reported that it was somewhere approximating the superior orbital fissure when viewed from the coronal view.

In this study, a 9.2-year-old child was included. Although this was a single sample, it did not have a significant impact on the results for the reasons following. First, the 3-dimensional changes of the ZMC of the sample were similar to those of other patients in the study. Second, the child was young, and MARME was only applied for a short period of about 30 days, so it is unlikely that facial growth affected the outcome.

Table VII. Correlation between the amount of CR6 expansion and changes in x, y, and z coordinates of the landmarks (n = 15)

		Amount of CR6 expansion	*ΔANS(x)*	*ΔPNS(x)*	*ΔZ(x)*	*ΔAlare(x)*	*ΔJ(x)*	*ΔA(x)*	*ΔEctomolare(x)*	*ΔEctocanine(x)*
Amount of CR6 expansion	Pearson correlation	1	0.430	0.464	0.419	0.409	0.282	0.412	0.601*	0.779†
	Sig (2-tailed)		0.110	0.082	0.120	0.130	0.309	0.127	0.018*	0.001†
		Amount of CR6 expansion	ΔANS(y)	ΔPNS(y)	ΔZ(y)	ΔAlare(y)	ΔJ(y)	ΔA(y)	ΔEctomolare(y)	ΔEctocanine(y)
Amount of CR6 expansion	Pearson correlation	1	0.004	0.508	0.126	0.690†	−0.143	0.295	0.350	0.170
	Sig (2-tailed)		0.989	0.053	0.655	0.004†	0.610	0.286	0.202	0.545
		Amount of CR6 expansion	ΔANS(z)	ΔPNS(z)	ΔZ(z)	ΔAlare(z)	ΔJ(z)	ΔA(z)	ΔEctomolare(z)	ΔEctocanine(z)
Amount of CR6 expansion	Pearson correlation	1	0.367	0.099	−0.131	0.190	0.143	0.075	0.413	0.047
	Sig (2-tailed)		0.178	0.726	0.641	0.498	0.611	0.791	0.126	0.869

Pearson correlation test was performed because of the normality of the data.
CR6 expansion meant the change of distance between the center of resistance of the maxillary first molars.
*P <0.05; †P <0.01.

Leonardi et al[23] reported that RME produced a significant bony displacement by disrupting the circummaxillary sutures. Ghoneima et al[24] suggested that forces resulting from RME had an effect primarily on the anterior craniofacial sutures such as intermaxillary and maxillary frontal nasal interfaces rather than on the posterior craniofacial structures such as the zygomatic interface. Bazargani et al[25] reported that the circummaxillary sutures appeared to be affected by RPE, but the changes were overall small, that is, between 0.30 and 0.45 mm, and they also reported that sutures further away from the maxilla showed a lower degree of disarticulation. In this study, it was noted that the circummaxillary and midpalatal sutures were affected by the MARME appliance. Although the changes in width of the circummaxillary sutures were not evaluated statistically, we found that the intermaxillary, frontonasal, frontomaxillary, nasomaxillary, and internasal sutures showed larger changes in width than the sutures articulated with zygomatic bone. There was little change in the width of the pterygomaxillary junction.

To understand the expansion pattern of the ZMC after RME, one should notice the articulation between the sphenoid bone and posterior region of the ZMC. Melsen and Melsen[26] reported that owing to increased rigidity of the posterior palatine area because of the change in its morphology with aging, disarticulation of the palatal bone from the pterygoid process was possible only when accompanied by a fracture of the interdigitated osseous surfaces in patients older than late juveniles. Holberg[27] reported that the aspects of deformation of the pterygoid process during RME were similar in youth and in adults and that the stresses on the sphenoid bone increased with aging and amount of expansion. Jafari et al[28] reported that the inferior region of the pterygoid process expanded laterally with hemimaxillae, but that the superior region of pterygoid process was hardly affected. Gautam et al[22] suggested the need for surgical severance of the pterygomaxillary junction because of the high stress on this area with lateral displacement of the pterygoid process during RME resulting in the potential for microfractures, which leads to possible injuries on neural and vascular structures. However, Stepanko and Lagravère[29] reported no clinically significant changes in the sphenoid bone after RME in both their tooth-anchored group and bone-anchored group.

In this study, a similar phenomenon in the pterygoid process was detected with superimposed CBCT images. The inferior part of the pterygoid process expanded laterally with the ZMC, and the superior part was barely affected with respect to its position after MARME. Because the sphenoid bone contains a lot of important neural and vascular structures, the skeletal effects after RME on this region might be critical, so they should be evaluated thoroughly to prevent any complications.

In this retrospective study, skeletal response and the expansion pattern of the ZMC after MARME were evaluated. Further studies with a larger sample size are needed to identify the long-term skeletal effects of MARME on the circummaxillary sutures, especially the pterygomaxillary junction and the bending displacement of the pterygoid plate and its possible rebound. Also, future studies with control groups are needed to evaluate the skeletal response of the ZMC objectively.

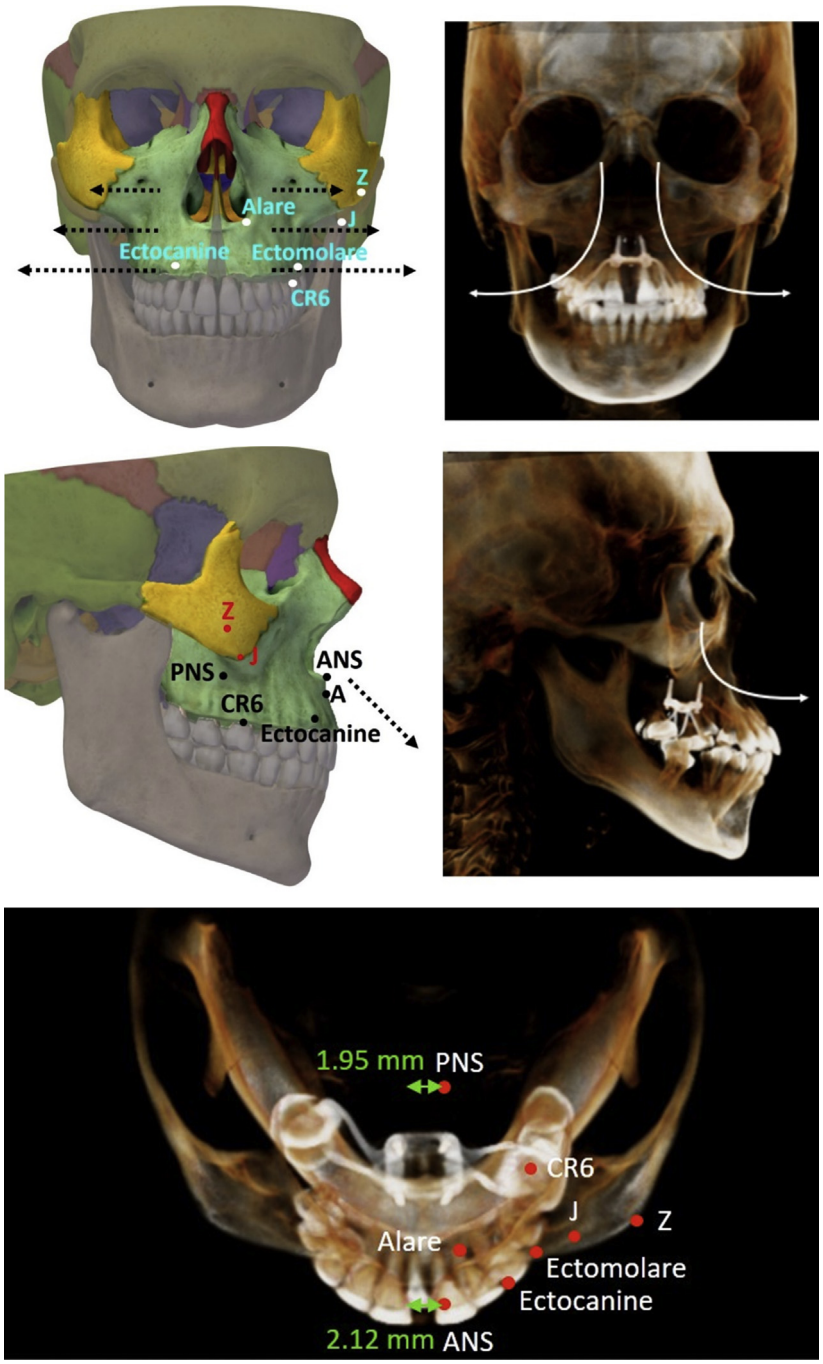

Fig 4. Skeletal expansion pattern of ZMC following MARME.

CONCLUSIONS

Skeletal effects of the ZMC after MARME were evaluated with CBCT images. From this study, we observed the following:

1. In the transverse dimension, the expansion of the ZMC was greater in the lower than in the upper portion and palatal expansion was similar in the anteroposterior portion.
2. In the sagittal and vertical dimensions, the ZMC showed forward and downward displacement, the posterior portion of the ZMC was displaced further downward than the anterior portion and the portion closer to the midsagittal plane was displaced further downward.

REFERENCES

1. Haas AJ. Rapid expansion of the maxillary dental arch and nasal cavity by opening the midpalatal suture. Angle Orthod 1961;31: 73-90.
2. Haas AJ. The treatment of maxillary deficiency by opening the midpalatal suture. Angle Orthod 1965;35:200-17.
3. Sandikçioðlu M, Hazar S. Skeletal and dental changes after maxillary expansion in the mixed dentition. Am J Orthod Dentofacial Orthop 1997;111:321-7.
4. Bell RA, LeComte EJ. The effects of maxillary expansion using a quad-helix appliance during the deciduous and mixed dentitions. Am J Orthod 1981;79:152-61.
5. Baccetti T, Franchi L, Cameron CG, McNamara JA Jr. Treatment timing for rapid maxillary expansion. Angle Orthod 2001;71:343-50.
6. Melsen B. Palatal growth studied on human autopsy material. A histologic microradiographic study. Am J Orthod 1975;68:42-54.
7. Suri L, Taneja P. Surgically assisted rapid palatal expansion: A literature review. Am J Orthod Dentofacial Orthop 2008;133:290-302.
8. Lee KJ, Park YC, Park JY, Hwang WS. Miniscrew-assisted nonsurgical palatal expansion before orthognathic surgery for a patient with severe mandibular prognathism. Am J Orthod Dentofacial Orthop 2010;137:830-9.
9. Carlson C, Sung J, McComb RW, Machado AW, Moon W. Microimplant-assisted rapid palatal expansion appliance to orthopedically correct transverse maxillary deficiency in an adult. Am J Orthod Dentofacial Orthop 2016;149:716-28.
10. Park JJ, Park YC, Lee KJ, Cha JY, Tahk JH, Choi YJ. Skeletal and dentoalveolar changes after miniscrew-assisted rapid palatal expansion in young adults: A cone-beam computed tomography study. Korean J Orthod 2017;47:77-86.
11. Chung CH, Font B. Skeletal and dental changes in the sagittal, vertical, and transverse dimensions after rapid palatal expansion. Am J Orthod Dentofacial Orthop 2004;126:569-75.
12. Habeeb M, Boucher N, Chung CH. Effects of rapid palatal expansion on the sagittal and vertical dimensions of the maxilla: A study on cephalograms derived from cone-beam computed tomography. Am J Orthod Dentofacial Orthop 2013;144:398-403.
13. Silva Filho OG, Villas Boas MC, Capelozza Filho L. Rapid maxillary expansion in the primary and mixed dentitions: a cephalometric evaluation. Am J Orthod Dentofacial Orthop 1991;100:171-9.
14. Yılmaz A, Arman-Özçırpıcı A, Erken S, Polat-Özsoy Ö. Comparison of short-term effects of mini-implant-supported maxillary expansion appliance with two conventional expansion protocols. Eur J Orthod 2015;37:556-64.
15. Brunetto DP, Sant'Anna EF, Machado AW, Moon W. Non-surgical treatment of transverse deficiency in adults using Microimplant-assisted Rapid palatal Expansion (MARPE). Dent Press J Orthod 2017;22:110-25.
16. Cho HJ. A three-dimensional cephalometric analysis. J Clin Orthod 2009;43:235-52: discussion 235; quiz 273.
17. Sarver DM, Johnston MW. Skeletal changes in vertical and anterior displacement of the maxilla with bonded rapid palatal expansion appliances. Am J Orthod Dentofacial Orthop 1989;95:462-6.
18. Vassar JW, Karydis A, Trojan T, Fisher J. Dentoskeletal effects of a temporary skeletal anchorage device-supported rapid maxillary expansion appliance (TSADRME): A pilot study. Angle Orthod 2016;86:241-9.
19. Lee KG, Ryu YK, Park YC, Rudolph DJ. A study of holographic interferometry on the initial reaction of maxillofacial complex during protraction. Am J Orthod Dentofacial Orthop 1997;111:623-32.
20. Braun S, Bottrel JA, Lee KG, Lunazzi JJ, Legan HL. The biomechanics of rapid maxillary sutural expansion. Am J Orthod Dentofacial Orthop 2000;118:257-61.
21. Baldawa RS, Bhad WA. Stress distribution analysis during an intermaxillary dysjunction: A 3-D FEM study of an adult human skull. Ann Maxillofac Surg 2011;1:19-25.
22. Gautam P, Valiahtan A, Adhikari R. Stress and displacement patterns in the craniofacial skeleton with rapid maxillary expansion: a finite element method study. Am J Orthod Dentofacial Orthop 2007;132:5.e1-11.
23. Leonardi R, Sicurezza E, Cutrera A, Barbato E. Early post-treatment changes of circummaxillary sutures in young patients treated with rapid maxillary expansion. Angle Orthod 2011;81:36-41.
24. Ghoneima A, Abdel-Fattah E, Hartsfield J, El-Bedwehi A, Kamel A, Kula K. Effects of rapid maxillary expansion on the cranial and circummaxillary sutures. Am J Orthod Dentofacial Orthop 2011;140: 510-9.
25. Bazargani F, Feldmann I, Bondemark L. Three-dimensional analysis of effects of rapid maxillary expansion on facial sutures and bones. Angle Orthod 2013;83:1074-82.
26. Melsen B, Melsen F. The postnatal development of the palatomaxillary region studied on human autopsy material. Am J Orthod 1982;82:329-42.
27. Holberg C. Effects of rapid maxillary expansion on the cranial base—an FEM-analysis. J Orofac Orthop 2005;66:54-66.
28. Jafari A, Shetty KS, Kumar M. Study of stress distribution and displacement of various craniofacial structures following application of transverse orthopedic forces—a three-dimensional FEM study. Angle Orthod 2003;73:12-20.
29. Stepanko LS, Lagravère MO. Sphenoid bone changes in rapid maxillary expansion assessed with cone-beam computed tomography. Korean J Orthod 2016;46:269-79.